CHAPTER 2

DETERMINATION OF SURFACE FREE ENERGIES OF TALC FROM CONTACT ANGLES MEASURED ON FLAT AND POWDERED SAMPLES

2.1 INTRODUCTION

The surface free energies and their components between two interacting surfaces are extremely important since not only do they dictate the strength of interaction, but also control processes like the stability of aqueous colloidal suspensions, the dynamics of molecular self-assembly, wetting, spreading, deinking and adhesion [1-4]. Many of the mineral processing techniques, e.g. froth flotation, selective flocculation, filtration and thickening also depend on the interfacial interactions between solid and liquid, essentially water. These interactions are mainly controlled by the interfacial surface tensions between two phases. The characterization of the surface properties and especially the surface free energy components of the solids are, therefore, recognized as the key to understanding the mechanism of surface-based phenomena.

Talc is used for various applications, including paper coatings, pitch control, ceramics manufacture, paint, plastics, cosmetics, etc. The market potentials of the various talc products depend on the surface properties of the mineral, which in turn vary with the ore type, processing methods, particle size, surface treatment, etc. It has been recognized that the characterizing the talc based on its surface properties (e.g., acid-base characterization, hydrophobicity-hydrophilicity, electrokinetic properties) are vitally important for defining suitable applications and developing new markets.

Talc, as a mineral, has unique surface properties. Particles of talc have the shape of platelets due to the layer structure of the mineral. It is well known that the basal surfaces are hydrophobic, while the edge surfaces are hydrophilic (5-6). The hydrophobicity of the basal surfaces arises from the fact that the atoms exposed on the surface are linked together by siloxane (Si-0-Si) bonds and, hence, do not form strong hydrogen bonds with water. The edge surfaces, on the other hand, are composed of hydroxyl ions, magnesium, silicon and substituted cations, all of which undergo hydrolysis. As a result, the edges are hydrophilic, and can form strong hydrogen bonds

with water molecules and polar substances [7-10]. In many of the industrial applications, this dual surface property of the mineral plays an important role. In the paper industry, for pitch and sticky control applications, the hydrophilic property of the edges allows the particles to be dispersed in aqueous media, while the hydrophobic property of the basal surfaces attract the sticky hydrophobic substances present in wood pulp.

For filler applications, proper control of the adhesion between talc and polymer matrix is important in controlling the property of the composite material. In general, stronger filler-matrix interactions result in improved processability, impact strength, and surface quality, while too weak interactions lead to decreased strength and increased deformability of the composite [10]. As a means of controlling the filler-matrix interactions, minerals are treated with appropriate surfactants [11, 12]. Acid-base interactions also play a crucial role in controlling these interactions. The knowledge of surface free energy components of talc and pitch and hydrophobic stickies or polymers, originating from different kinds of intermolecular forces is, therefore, very useful for understanding the surface interaction mentioned above.

The standard approach used for determining the surface free energies of solids and the interfacial surface free energies between interacting surfaces has been through wetting experiments. Specifically, the contact angle method has been widely used to characterize the surface properties of solids [13-18]. Contact angle value is more often used as a measure of the surface hydrophobicty [19-23]. The higher the contact angle value, is the more hydrophobic the solid surface.

The contact angle measurements are easy to perform on a smooth flat surface, and there are several well-known techniques for measuring the contact angles of liquids on the flat surfaces. In many of the industrial applications, however, materials are used in powdered form. In such a case, it becomes difficult to obtain the value of contact angle for powdered surfaces. It is also unreliable and impractical to use the conventional contact angle measurement techniques for the characterization of fine powders such as fillers, pigments and fibers. Despite the difficulties associated with the contact angle measurements, some methods are available for determining the contact angles of powders [18].

The most commonly used technique for the measurement of contact angle on powders is the Washburn method, known as the capillary rise technique [24-26]. The thin layer wicking technique, which is also based on the Washburn equation, can also be used for the determination of contact angles on powdered surfaces [27, 28]. Even though these techniques are based on assumptions, to date they seem to be the most reliable techniques for the measurement of contact angles on powdered surfaces.

Alternatively, the contact angle of a powdered sample is measured by compressing it into a pellet. Some authors indicated that the pressed talc sample might have a different contact angle from that of loose powders because of the deformation of the upper layer particles during compression [18]. Surface roughness and the porosity of particles may also change on the pressed surface.

2.1.1 Van Oss-Chaudhury-Good Equation

Fowkes [29] proposed that the work of adhesion (W_a) between a liquid on a solid surface is given by:

$$W_{\mathrm{a}} = W_{\mathrm{ad}}^{\mathrm{d}} + W_{\mathrm{ad}}^{\mathrm{nd}} \qquad [2.1]$$

where W_a^d represents the contributions from dispersion (nonpolar) interactions, and W_a^{nd} represents the same from non dispersion (polar or ionic) interactions. Laskowski and Kitchener [30] suggested that all solids would be hydrophobic if W_{ad}^{nd}=0, i.e., if the surface is free of polar groups on which water molecules can be bonded.

In the last twenty years, significant advances have been made in the thermodynamic treatment of surface free energies, largely due to the pioneering work of Fowkes et al., [31-33] and van Oss, Chaudhury and Good [34-37]. According to these approaches the surface free energy of a phase *i* is given by:

$$\gamma_{\mathrm{i}} = \gamma_{\mathrm{i}}^{\mathrm{LW}} + \gamma_{\mathrm{i}}^{\mathrm{AB}} \qquad [2.2]$$

where γ_i^{LW} and γ_i^{AB} refer to the apolar and polar (acid-base) components of surface free energy, respectively. The former can be represented by the Lifshitz-van der Waals (or LW) interactions that include the dispersion (London), induction (Debye) and orientation (Keesom) components. The polar interactions are generally considered to be intermolecular interactions between Lewis acids (electron acceptor) and bases (electron donor) on the surface.

According to Van Oss-Chaudhury-Good (OCG) approach the surface free energy change upon two interacting surfaces (e.g. solid and liquid) is given by:

$$\Delta G_{SL} = -2\sqrt{\gamma_S^{LW}\gamma_L^{LW}} - 2\sqrt{\gamma_S^{+}\gamma_L^{-}} - 2\sqrt{\gamma_S^{-}\gamma_L^{+}} \qquad [2.3]$$

The changes in free energy associated with the solid liquid interaction is given by the following relation [38]:

$$\Delta G_{SL} = \gamma_{SL} - \gamma_S - \gamma_L \qquad [2.4]$$

Substituting Eq. [2.4] into Eq. [2.3], one obtains:

$$\gamma_{SL} = \gamma_S + \gamma_L - 2\left(\sqrt{\gamma_S^{LW}\gamma_L^{LW}} + \sqrt{\gamma_S^{+}\gamma_L^{-}} + \sqrt{\gamma_S^{-}\gamma_L^{+}}\right) \qquad [2.5]$$

which allows one to determine the interfacial surface tension of two interacting surfaces (e.g. water and talc). As shown, there are four unknowns for the calculation of γ_{SL}; the surface free energy components of solid, i.e., γ_S, γ_S^{LW}, γ_S^{+}, and γ_S^{-}. The surface free energy components of liquid are generally available in literature. The surface free energy components of solid can be determined by using van Oss-Chaudry-Good (OCG) equation that is derived as follows:

Work of adhesion or Gibbs free energy of interaction can be related to the interfacial energies through Young's equation [39],

$$\gamma_L \cos\theta = \gamma_S - \gamma_{SL} \qquad [2.6]$$

where γ_L is the surface tension of water and γ_{SL} is the interfacial tension between the solid and liquid.

Combining Eqs. [2.5] and [2.6],

$$-\Delta G_{SL} = \gamma_L (1 + \cos\theta) = W_{ad} \qquad [2.7]$$

Substituting Eq. [2.7] into Eq. [2.5], one obtains:

$$(1 + \cos\theta)\gamma_L = 2\left(\sqrt{\gamma_S^{LW}\gamma_L^{LW}} + \sqrt{\gamma_S^{+}\gamma_L^{-}} + \sqrt{\gamma_S^{-}\gamma_L^{+}}\right) \qquad [2.8]$$

which is a very useful information for characterizing a solid surface in terms of its surface free energy components, i.e., γ_S^{LW}, γ_S^{+}, and γ_S^{-}. To determine these values, it is necessary to determine contact angles of three different liquids of known properties (in terms of γ_L^{+}, γ_L^{-}, γ_L^{LW}) on the surface of the solid of interest. One can then set up three equations with three unknowns, which can be solved to obtain the values of γ_S^{LW}, γ_S^{+}, and γ_S^{-}. Table 2.1 gives a list of liquids that can be used for the contact angle measurements, along with the values of γ_L, γ_L^{LW}, γ_L^{+}, and γ_L^{-}.

If an apolar liquid is placed on the surface of a talc sample and its contact angle is measured, Eq. [2.8] can be reduced to:

$$(1 + \cos\theta)\gamma_L = 2\sqrt{\gamma_S^{LW}\gamma_L^{LW}}\,, \qquad [2.9]$$

because γ_L^{+} and γ_L^{-} are zero. Thus, Eq. [2.9] can be used to determine γ_S^{LW} from a single contact angle value, provided that the contact angle measurement is conducted with an apolar liquid of known γ_L and γ_L^{LW}. (In fact, $\gamma_L = \gamma_L^{LW}$, γ_L^{+} and γ_L^{-} are zero.) As the value of γ_S^{LW} is already estimated from Eq. [2.9], Eq. [2.8] can now be used to determine the values of γ_S^{+} and γ_S^{-} by solving two simultaneous equations.

Once the three surface tensions, i.e., γ_S^{LW}, γ_S^+, and γ_S^-, are known, the surface tension of the solid, γ_S, can be determined as follows:

$$\gamma_S = \gamma_S^{LW} + \gamma_S^{AB} \\ = \gamma_S^{LW} + 2\sqrt{\gamma_S^+ \gamma_S^-} \qquad [2.10]$$

The surface free energy, γ_S, is a material specific parameter which, when known for two materials, can be used to estimate the wettability, work of adhesion and the changes in the Gibbs free energy upon interaction.

2.1.2 Contact Angle Measurements

As has already been discussed, it is necessary to measure the contact angle (θ), if one wishes to characterize the surface of a solid in terms of its surface free energy components. Figure 2.1 shows that a finite contact angle is formed when a drop of liquid is brought into contact with a flat solid surface, the final shape of the drop depending on the relative magnitudes of the molecular forces that exist within the liquid (cohesive) and between liquid and solid (adhesive). Thus, the contact angle is a measure of the competing tendencies of the liquid drop and solid determining whether it spreads over the solid surface or rounds up to minimize its own area. For example, when a low surface energy liquid wets a solid surface, giving a zero contact angle, the molecular adhesion between solid and liquid is greater than the cohesion between the molecules of the liquid. On the contrary, liquids with high surface tension tend to give a finite (non-zero) contact angle, indicating that the cohesive force is greater than the energy of adhesion between liquid and solid [40]. The figure also illustrates the importance of acid-base interactions on the value of contact angle, hence on the magnitude of adhesion. The concept of the equilibrium of the surface forces is expressed mathematically by Young's equation (Eq. [2.6]).

Among the terms given in Young's equation (Eq. [2.6]), the only other measurable quantity appears to be γ_L along with the contact angle (θ). In fact, what is

measurable is γ_{LV}, the surface tension of the liquid against some vapor, either air or the equilibrium vapor of the liquid. It is generally assumed, however, that $\gamma_L \approx \gamma_{LV}$ [41].

One of the major problems in the use of Young's equation is that its assumption of $\gamma_S \approx \gamma_{SV}$. This may or may not be the case, depending on the experimental conditions. In particular, the surface free energy of solid can significantly be reduced as a result of the adsorption of the vapors of the wetting liquid (at saturation) onto the solid surface. When the solid surface is in equilibrium with the liquid vapor, the reduction of the surface free energy of the solid due to the vapor adsorption is termed the equilibrium spreading pressure, π_e, and hence its addition into Eq. [2.6] leads to the modified Young equation:

$$\gamma_L \cos\theta = \gamma_S - \gamma_{SL} + \pi_e \qquad [2.11]$$

where $\pi_e = \gamma_S - \gamma_{SV}$. Thus, the reduction in the value of the ideal surface free energy of a solid (γ_S) due to the adsorption of liquid vapor onto the solid surface can be measured as a function of π_e [42].

The equilibrium spreading pressure may be measured experimentally from the adsorption isotherms for the vapors of the liquid on the solid surface, $\Gamma = \Gamma(p)$, where p is the partial pressure of the vapors of the liquid, using the Gibbs adsorption equation [43]:

$$\pi_e = \gamma_S - \gamma_{SV} = RT \int_0^P \Gamma d \ln P \qquad [2.12]$$

where P is the saturation vapor pressure of the liquid. However, the measurement of π_e is cumbersome and is not, in general, a simple task on a macroscopic solid surface and its theoretical estimation is difficult.

It is, therefore, common among the investigators to assume that π_e should be negligible for all cases in which the contact angle is finite, i.e., for so-called smooth, homogenous, hydrophobic low energy surfaces [27, 44]. Fowkes et al [44] studied the

possibility of spreading pressures arising with high-energy liquids deposited on low-energy solids, and found that this did not occur. On the other hand, when the vapor of a low-energy liquid could interact with a somehow higher-energy solid surface, the effect of resulting positive spreading pressure caused an increase in the contact angle of water on that solid surface, which allowed the determination of π_e [44]. Van Oss et al. [27] also showed by conducting thin layer wicking measurements, with non-spreading liquids (i.e. $\gamma_L > \gamma_S$ and $\cos\theta < 1$) neither spreading nor pre-wetting takes place on low-energy solid surfaces. Thus, it appears not to be justified to take the equilibrium spreading pressures into account, under non-spreading conditions.

It has been shown, however, that substantially positive π_e values could exist with non-spreading liquids [45, 46]. Busscher et al [45] studied the adsorption of water and propanol on various solid surfaces using ellipsometry technique. The authors showed that even when $\gamma_L > \gamma_S$, spreading pressures can have a considerable effect on the contact angle value. They correlated the adsorption of water and propanol on solid surfaces with equilibrium spreading pressures. They found that the equilibrium spreading pressures are in the same order of magnitude for water and for propanol on both high- and low-energy surfaces. However, it is well known that the spreading behavior of low-energy liquids (e.g, propanol, $\gamma_{propanol} = 23.7$ mJ/m^2) differs fundamentally from the high-energy liquids (e.g., water, $\gamma_{water} = 72.8$ mJ/m^2), especially on solids with $\gamma_S \approx 35 \pm 10$ mJ/m^2 (Fowkes et al., [44]). Fowkes et al (44) showed that the vapor of water does not spread over low energy polymers, while cyclohexane vapor spreads over the polymer surface. Thus, the correlation between the ellipsometric results and the equilibrium spreading pressures, particularly when using alcohol-water mixtures, must be regarded as questionable.

2.1.2.1 On Flat Surfaces

There are several different methods of measuring contact angles on the flat solid surfaces. The easiest are *the sessile drop* and *the captive bubble* techniques. In the sessile drop technique, a liquid droplet is places on the surface of a solid of interest and the angle is measured through the liquid phase (Figure 2.1).

In the captive bubble technique, the solid surface is immersed in a liquid and an air bubble (or a drop of another liquid) is brought to the solid/liquid interface. If the

surface is hydrophobic, the bubble will stick to the surface. The angle between the surface of the solid and the air bubble is then measured through the liquid phase.

A third method consists of dipping a solid into a liquid and measure the height *(h)* of a liquid rising along the surface. If the surface tension *(γ)* and the density *(ρ)* of the liquid are known, one can use the following equation [47] to calculate the contact angle *θ*:

$$1-\sin\theta=\frac{h^2\rho g}{2\gamma}, \qquad [2.11]$$

where *g* is the gravitational acceleration. This method, which is known as *Wilhelmy plate* method, also requires that a flat surface is available.

2.1.2.2 On Powdered Surfaces

Capillary rise and thin layer wicking techniques, both of which based on the Washburn equation, can be used to determine the contact angles when a solid exists only in powdered form. In the capillary rise technique, a powdered solid is packed into the capillary tubing, which is subsequently immersed into a liquid of known surface tension. The liquid will rise through the capillaries formed in between the particles within the tubing. The distance *l* traveled by the liquid as a function of time *t* is measured. If one knows the mean radius r^* of the capillaries present in the tubing, the contact angle can then be calculated using the Washburn equation [48, 49]:

$$l^2=\frac{\gamma_{LV}r^*t\cos\theta}{2\eta}, \qquad [2.12]$$

where η is the viscosity of the liquid. One can determine r^* with a liquid which completely wets the powder, i.e., θ=0. This can be done by using low-energy apolar liquids such as hexane, heptane, octane, benzene etc. which spread over the solid surface without forming a finite contact angle [28]. The capillary rise technique has frequently been used on mineral powders (24-26).

One problem with this technique might be the uncertainty associated with determining r^*. There is no guarantee that the value of r^* determined with a completely wetting liquid is the same as that determined by a less than completely wetting liquid. Reproducibility and repeatability of test results also depend on the shape and size of the particles. It has been stated that monosized and spherical particles give more reproducible results [27]. It should be mentioned here that the method of using the Washburn equation gives only advancing contact angles rather than equilibrium contact angles.

In the thin layer wicking method, a powdered sample is deposited on a microscopic glass slide in the form of aqueous slurry on which a thin layer of the powdered mineral has been formed. After drying the sample, one end of the glass slide is immersed vertically in a liquid. The liquid will start to creep up the slide through the capillaries formed between the particles deposited on the glass surface. The velocity at which a liquid creeps up the slide is measured, and then converted to a contact angle using the Washburn equation (Eq. [2.12]) [27, 28].

Alternatively, the particles can be pelletized under pressure and contact angle measurements can be made in a similar manner described above for flat surfaces. However, compression of particles into a pellet presents problems such as liquid absorption, porosity, and considerable surface roughness. Also, treatment of the pellet's surface in the same fashion as that of flat surfaces should be avoided due to the same problems mentioned above. For these reasons, the measured contact angles on pelletized surfaces might significantly differ from those obtained on flat surfaces [18].

It was the primary objective of the present work to study the possibility of measuring the contact angles on powdered talc samples and to compare them with those obtained on polished flat talc samples. This will allow the surface free energy parameters of solid surfaces to be calculated from the measured contact angles. In order to meet this objective, contact angle measurements were conducted on i) flat samples using the sessile drop and Wilhelmy plate techniques, and ii) powdered samples using the capillary rise and thin layer wicking techniques. The results were evaluated on the basis of acid-base interactions that play an important role in two interacting surfaces. It is obvious that the knowledge of surface free energy parameters and the change in surface free energy

between two interacting surfaces will be helpful in understanding the surface characteristics of materials and the molecular origin of the adhesion. The effect of grinding, and hence, the particle size, on the surface properties of talc were also discussed based on the contact angle measurements. The samples were also subjected to ESCA measurements to determine how elemental composition can affect the surface acidity/basicity or hydrophobicity of talc. It was also aimed to demonstrate the effect of equilibrium spreading pressure by determining contact angles after the exposure of the powdered talc samples to water vapor for 24 hours.

2.2 EXPERIMENTAL

2.2.1 Samples

The run-of-mine (ROM) samples from the Montana and Vermont deposits were received in buckets from Luzenac America. They were crushed to -50 mm using a hand-held hammer. The crushed samples were divided into two parts. One part was kept for contact angle measurements using the sessile drop and Wilhelmy plate techniques, while the other part was ground to -150 μm using an agate mortar and pestle. The ground samples were used for contact angle measurements using the capillary rise and thin layer wicking techniques.

A number of powdered samples were also received from Luzenac America, which were named i) Yellowstone (d_{50}=12.5 μm), ii) Mistron-100 (d_{50}=3.5 μm), iii) Mistron Vapor-P (d_{50}=3.0 μm), and iv) Select-A-Sorb (d_{50}=3.4 μm). They were used for the characterization studies as received.

2.2.2 Liquids

The contact angle measurements were conducted using apolar and polar liquids:

Apolar Liquids:	hexane, heptane, octane, decane, dodecane, cyclohexane, benzene, methylene iodide and 1-bromonaphthalene
Polar liquids:	water, glycerol, formamide and ethylene glycol.

The former interacts with talc through Lifshitz-van der Waals interactions, while the latter interacts with talc through hydrogen bonding (acid-base interactions).

All of the organic liquids used in the present work were HPLC grade (>99.5% purity) and dried overnight over 3 to 12 mesh Davidson 3-A molecular sieves before use. 1-Bromonaphthalene, methylene iodide, hexane, heptane, octane, decane and dodecane were obtained from Aldrich Chemical Company; while formamide, glycerol, ethylene glycol, cyclohexane, and benzene were purchased from Fisher Scientific. All experiments were conducted using Nanopure water produced from a Barnstead Nanopure II water purification system.

2.2.3 Contact Angle Measurements

2.2.3.1 On Flat Surfaces

Large pieces of run-of-mine talc samples were cut to plates with dimensions of approximately 20x15x1.5 mm using a diamond saw (Buehler, Isomet). Each plate was first polished with different grades of abrasive paper (Buehler 60, 400 and 600 grit), and then with alumina powder (Buehler 0.3 and 0.05 μm) on a rotating wheel polisher (Buehler, Ecomet III). After the final polishing, the plates were subjected to ultrasonic vibration to remove the fine abrasive particles from the surface. The samples were rinsed with ethanol and Nanopure water, and then air-dried before contact angle measurements.

The sessile drop technique was used to measure the equilibrium contact angles of different liquids listed in Table 2.1. In this technique, a small drop of liquid (2-4 mm diameter) was placed on the surface of a polished talc plate using a microliter syringe, and the contact angle was measured through the liquid phase using a Ramé-Hart goniometer (Model 100), which was equipped with a thermostatted environmental chamber.

Contact angles of a polished talc surface were also measured using the Wilhelmy plate technique by means of a KSV-Sigma70 contact angle/surface tensio-meter. Advancing and receding contact angles were obtained by moving the substrate into and out of the liquid at a speed of 0.6-0.7 mm/min. The contact angle values obtained during the first immersion were used. This equipment was equipped with a temperature control

device, so that contact angles could be measured at different temperatures. Unless otherwise stated, all contact angle measurements performed at 20 ±2 ^{o}C.

2.2.3.2 On Powdered Surfaces

a) Capillary Rise Technique

The capillary rise technique was used to measure the contact angles of various powdered talc samples using the Washburn equation (Eq. [2.12]). The Montana and Vermont talc samples that were used in these measurements were prepared by grinding the large pieces of the samples, while the other powders were used as received. In these experiments, a known amount of powder was placed in glass tubing with an inner diameter of 6.5 mm, by manual tapping. The bottom part of the tube was closed with a glass frit. The tube was always filled to the same height with the same weight of sample for a uniform and constant package of the particles. The packed tube was then placed upright position in the wetting liquid, and the wetting height was measured as a function of time. Before starting the next liquid, the tube was wetted with the liquid studied, rinsed with acetone and dried in an oven at 105 ^{o}C before packing with the powder. The measurements were conducted three to five times with a given sample and a liquid in order to check reproducibility.

The effective capillary radius (r^*) was determined using heptane, which was found to completely wet the talc samples. Once the value of r^* was obtained, it was then possible to calculate the value of the contact angle for a given liquid on the powdered talc surface using the Washburn equation. In the capillary rise experiments, 1-bromonaphthalane, water and formamide were used for contact angle measurements.

b) Thin Layer Wicking Technique

An aqueous suspension of talc (5% weight by volume) was prepared by dispersing a known amount of sample in distilled water, while the suspension was agitated to keep particles in suspension. Approximately 3 ml of the suspension was withdrawn with a pipette and sprayed over a glass slide (1 x 3”). Upon evaporating the water at room temperature, the samples were further dried in an oven at 110 ^{o}C to remove

any residual pore water that might interfere with the measurements. The residual water can dilute the wicking liquids and change their surface tensions and viscosities. Following this procedure, a uniform thin layer of powdered talc firmly adhering to the glass was obtained. The coated slides were then stored in a desiccator until required.

The wicking experiments were performed by immersing the coated glass slides in the vertical position to a depth of about 5 mm in a test liquid using a cylindrical glass container with a gas-tight ground-glass stopper. Before actual immersion, the coated slide was kept inside the closed container for about one hour, to allow the powder to come to equilibrium with the vapor of the wicking liquid [50]. The slide was then immersed into the liquid, and the vertical movement of the liquid through the particle bed was observed. After the liquid had traveled to the required distance (e.g. between 1 and 5 cm), the experiment was stopped by removing the slide from the glass container. With low-energy liquids typically the wetting took from 2 to 10 minutes, whereas it took as long as 35 minutes with high-energy liquids. With each sample, the tests were repeated at least three times.

The value of r^* in the Washburn equation was determined using completely spreading liquids (apolar) such as hexane, heptane, octane, decane and dodecane. In this case, it was considered that $\cos\theta=1$. For each talc powder, the $2\eta l^2/t$ vs. γ_L for alkanes yielded a straight line whose slope is the mean pore radius (r^*). Once the value of r^* was obtained, it was then possible to calculate the value of contact angle using the Washburn equation (Eq. [2.12]). In the present work, water, formamide, ethylene glycol, methylene iodide and 1-bromonapthalene were used as the wetting liquids.

In order to study the effect of humidity and the equilibrium spreading pressure (π_e) on the surface properties of the talc powders, the dried glass slides coated with the layer of particles were placed in a desiccator for 24 hrs that was filled with distilled water. The slides were then subjected to the thin layer wicking experiments as described above. In these tests, only Select-A-Sorb powder was subjected to the surface humidification to study the effect of equilibrium spreading pressure using the thin layer wicking method.

2.3 RESULTS AND DISCUSSION

2.3.1 Contact Angles

The equilibrium contact angles measured using the sessile drop technique on the flat surfaces of Montana and Vermont samples are given in Table 2.2. As shown, the water contact angles obtained for the Montana and Vermont talc samples are very close, Montana talc giving a slightly higher value. The other liquids tested also gave closer values of contact angles. The highest values were obtained with water.

Table 2.3 shows the results of the advancing and receding contact angles for water, formamide and methylene iodide measured on the flat talc surfaces using Wilhelmy plate technique. As shown, there is a contact angle hysteresis, suggesting a chemical or morphological heterogeneity of the surface. Note also that the advancing contact angles measured on the flat Montana surface are higher than those obtained on the Vermont talc sample. The data given in this table suggests that the Montana talc surface is more hydrophobic than the Vermont talc surface.

The results given in Table 2.2 and 2.3 demonstrate that the advancing contact angles measured on the flat samples using the Wilhelmy plate technique are higher than those measured using the sessile drop technique with either of the liquids used. The reason was that the contact angles were equilibrium contact angles measured with a goniometer while the advancing (and receding) contact angles were measured with the Wilhelmy plate technique. It can be expected that the equilibrium contact angles should remain somewhere in between the advancing and receding contact angles as suggested from the following equation (51):

$$\theta_{av} = \frac{\theta_a + \theta_r}{2} \qquad [2.13]$$

where θ_{av} is the average, θ_a the advancing and θ_r the receding contact angle, respectively. In the present work, the values of equilibrium contact angle measured are close to the average values of advancing and receding contact angles.

In the capillary rise experiments, for all powders, linear plots of l^2 *vs.* t were obtained. Figure 2.2 shows the wetting results obtained using the capillary rise method

with the powdered Montana talc sample with a size range of 150 x 53 μm. The values of $r^* cos\theta$ for each talc powder were calculated from the slops of the lines, the viscosities and the surface tensions of the liquids (Eq. [2.12]). The values of liquid surface tension and viscosities, given in Table 2.1, were used for the calculations [27-28, 52]. Among the liquids tested, the highest value of $r^* cos\theta$ was obtained when heptane was used as the wetting liquid for all the powdered talc samples studied. Therefore, it was chosen as the completely wetting liquid (i.e., θ=0). This allowed one to calculate r^*, which in turn allowed calculating contact angles for the other liquids, i.e., water, formamide and 1-bromonaphthalene.

The values of the contact angles of the various powdered talc samples measured using the capillary rise technique are given in Table 2.4. As shown, Select-A-Sorb powder gave a water contact angle value of 89.9^o, while the contact angles of other powders were in the range of 67 to 78^o. The contact angle values obtained using other liquids exhibited similar trend i.e., Select-A-Sorb gave the highest contact angles. It should be noted here that the reproducibility of the capillary rise technique was poor. There was as much as 5.3^o deviation from the average value of water contact angle. The same deviation from the average value was also observed with the other liquids. It is likely that the pore radius (r^*) changed with different liquids. This is possible because degree of wetting should affect the packing density of the fine particles. In this regard, the capillary rise technique may not be reliable with the samples containing ultrafine particles.

Thin layer wicking experiments yielded linear plots of l^2 *vs.* t, for all powders studied, which was similar to the capillary rise tests. In Figure 2.3, a plot of l^2 vs. t is given for alkanes (hexane, heptane, octane, decane and dodecane) on Select-A-Sorb talc powder, while the same is given in Figure 2.4 for the other wetting liquids used, e.g. 1-bromonaphthalene, methylene iodide, water, formamide and ethylene glycol. The value of r^* in the Washburn equation (Eq. [2.12]) for each talc powder have been obtained from the plots of $2\eta l^2/t$ vs. γ_L using alkanes as the wicking liquids. A sample plot for determining r^* using alkanes in the thin layer wicking experiments is given in Figure 2.5 for Select-A-Sorb talc powder. As shown, the plot of $2\eta l^2/t$ vs. γ_L yields a straight line whose slope is gives r^* [27].

The values of average particle size (d_{50}) and mean pore radius (r^*) for various talc powders are given in Table 2.5. As shown, the value of r^* determined from thin layer wicking measurements is mainly dependent on the particle size, but other variables such as the origin of talc ore, aspect ratio, surface treatment etc. may also effect the magnitude of r^*. Generally, as the particle size is finer, the value of r^* becomes smaller. For example, the value of r^* is 286.0 nm for Mistron-100 powder which has a d_{50} of 3.5 μm, whereas it is 626.7 nm for Yellowstone talc whose mean particle size is 12.5 μm.

Table 2.5 also compares the values of mean pore radius (r^*) of the run-of-mine Montana and Vermont talc samples that were ground in our laboratory. In the thin layer wicking tests, it was possible to obtain a homogenous layer of particles on the glass slide with the Montana talc even if the upper particle size was as large as 53 μm. However, it was not possible to obtain a smooth and homogenous layer of particles with the Vermont talc when using the same particle size range, e.g. 53 μm x 0. The particles of Vermont talc tend to break down along the basal planes and in a monosized manner because of its platy nature. During the deposition, the large and platy particles formed patches and bumps on the glass slide, which did not allow the wetting rise to be read accurately during the wicking experiments. It was, therefore, decided to further grind the Vermont talc below 38 μm. As a result, a homogenous layer of particles on the glass slide was successfully obtained. As shown in Table 2.5, although the upper particle size of the Montana talc used in the thin layer wicking experiments was larger than the Vermont talc sample, the value of r^* was much smaller. The obtained values of r^* were 1333.0 nm and 3093.0 nm for the Montana and Vermont talc samples, respectively. These results show clearly how the platy nature or large particle size might affect the porosity and formation of the thin layer of particles deposited on the glass slide.

The advancing contact angles of various liquids on the powdered talc samples obtained from thin layer wicking measurements are given in Table 2.6. As shown, the values of advancing water contact angles for various talc powders were in the range of 82 and 89.4^o. The data suggest that the most hydrophobic powder is Select-A-Sorb, with Mistron-100 powder being the most hydrophilic. It should be noted that the reproducibility of the test results using the thin layer wicking technique is better than those obtained using the capillary rise technique. It should be also noted that the

difference in the value of contact angles between various powders is not as pronounced as that obtained using the capillary rise technique. The difference between the lowest and highest value of water contact angles for various powders was 22^o (89.9^o for Select-A-Sorb powder and 67^o for Yellowstone powder) in the capillary rise tests, whereas it was only 7.4^o in the thin layer measurements (see Table 2.4 and 2.6). The same can be said of the other test liquids used in the contact angle measurements.

The results presented in Tables 2.4 and 2.6 show that using the thin layer wicking technique for the determination of the contact angles on powders is superior to the capillary rise technique, i.e., the reproducibility of test results is better. Another and maybe even more important advantage would be that the problems associated with ultrafine particle size distribution are eliminated. However, the thin layer wicking technique is restricted to the upper particle size of approximately 45-53 μm. When the particle size is large, it is difficult to obtain a smooth, homogenous layer of particles on the surface of glass slide. Larger particles tend to form patches and bumps on the glass surface.

Table 2.7 compares the flat and powdered surfaces in terms of their advancing contact angles obtained using water and formamide as the test liquids. As shown, the contact angles measured by capillary rise and thin layer wicking techniques on the powdered surfaces are invariably higher than those measured by using Wilhelmy plate technique on the flat surfaces. For example, the advancing water contact angle was 69.3^o on the flat Montana talc surface, whereas it became 82.3^o for powdered Montana talc surface that is in the size range of 150 x 53 μm. The contact angle further increased to 86.5^o when the particles became finer, e.g. 53 μm by 0. The contact angles of test liquids on the run-of-mine Vermont talc were increased in the same fashion as given in Table 2.7. It can also be seen from Table 2.7 that the values of contact angles measured using either water or formamide on both the flat and powdered Vermont talc surfaces were smaller than those obtained on the Montana talc sample.

A reasonable explanation for obtaining higher advancing water contact angles on the ground samples would be that the surface properties of talc are changed significantly because of mechanical grinding. More hydrophobic basal plane surfaces were exposed upon pulverization; as a result, water contact angle is increased. This is schematically

illustrated in Figure 2.6. The increase in the value of contact angles for the other test liquids can also be explained in the same sense, e.g. the surface free energy of talc was reduced after the grinding due to the creation of more basal surfaces as discussed in the following section.

In the present work, the measured values of advancing water contact angle on various powdered talc samples were in the range of 69 to 89.9^o (See Tables 2.4 and 2. 6). It has to be pointed out that the θ_a values for water reported in literature on flat talc surfaces are in the range from 62 to 81^o [5], while the θ_a values reported for powdered talc samples is approximately 76-79^o [28]. Hence, the contact angle data reported here is in agreement with what has been published in the literature, even though somewhat higher values of advancing water contact angles on the powdered samples were obtained in the present work. It can be expected that the origin of talc ore, surface preparation techniques, processing, particle size etc. may affect the surface hydrophobicity, and thus the value of the contact angle.

A series of contact angle measurements have been conducted on the Select-A-Sorb powder to determine the effect of exposure of particles to water vapor and to determine the effect of spreading equilibrium pressure (π_e). In these experiments, the particles were exposed to water vapor in a desiccator for 24 h. Table 2.8 compares the values of the contact angles for various liquids on the Select-A-Sorb powder that are determined using the thin layer wicking technique before and after the exposure of particles to water vapor. As shown, the contact angle values for all of the test liquids were somewhat decreased after the powder was exposed to the water vapor. The advancing water contact angle on the Select-A-Sorb powder was 89.4^o before the exposure to water vapor, whereas it reduces to 87.5^o after the exposure. The decrease in the value of water contact angle after the exposure is only 1.9^o. The difference between the measured contact angle values on the exposed and unexposed talc surfaces for the other test liquids was also small. The maximum decrease in the value of contact angle was observed with methylene iodide, exhibiting a reduction of 3.3^o. The results given in this table show that the effect of equilibrium spreading pressure of water on the talc surface is negligibly small as it is expected for low-energy hydrophobic surfaces [27, 44].

The results indicate that the vapors of high-energy water do not adsorb on the low-energy talc surfaces.

2.3.2 Surface Free Energies of Talc

The values of contact angles given in Table 2.2 for the sessile drop technique were used to calculate the Lifshitz-van der Waals (γ_S^{LW}), Lewis electron donor (γ_S^-) and electron acceptor (γ_S^+) components of the surface free energies on the Montana and Vermont talc samples using Eq. [2.8]. As discussed before, the calculation requires a set of three contact angles for three different liquids, along with their surface tension components. The values of γ_L^{LW}, γ_L^+, and γ_L^- for liquids were taken from the literature (See Table 2.1). Methylene iodide-water-glycerol or methylene iodide-water-formamide combinations were used to calculate the values of γ_S^{LW}, γ_S^- and γ_S^+ components of the surface free energy of talc samples. The results are shown in Table 2.9. Also shown in this table are the values of γ_S^{AB} ($=2\sqrt{\gamma_S^+\gamma_S^-}$) and γ_S calculated using Eq. [2.10] from the values of the surface free energy components. As shown, the surface free energy and its components calculated using the two liquid combinations stated above gave closer values of surface free energy components both on the Montana and Vermont talc samples, although one combination gives somewhat higher value of γ_S^- for both samples than the other.

Similar calculations were also made from the contact angle data reported for the Wilhelmy plate, capillary rise and thin layer wicking techniques. For a given talc surface, the advancing contact angles (θ_a) measured using three test liquids; i.e., water, formamide and methylene iodide (or 1-bromonaphthalene) were used for calculating the surface free energy components of talc surfaces. The advancing contact angle is generally considered to be the intrinsic contact angle of the surface with microscopic heterogeneity [53-55]. Based on the values of θ_a obtained for these liquids, Eq. [2.8] was solved simultaneously to obtain the values of the relevant surface free energy components.

Table 2.10 shows the surface free energy components of the flat Montana and Vermont talc samples that are determined from the Wilhelmy plate measurements. As

shown, the γ_S^{LW} and γ_S^{AB} components on the flat Vermont talc surface are higher than those obtained on the flat Montana talc surface. Also shown in the table are the values of γ_S^- and γ_S^+. As shown, the Vermont talc surface has a slightly higher value of γ_S^- than the Montana talc surface, whereas the γ_S^+ is essentially the same on both talc surfaces. The value of γ_S^- is, however, much higher both on the Vermont and Montana talc surfaces than the value of γ_S^+, suggesting that the talc surface is predominantly basic, while there are few acidic sites as well. Also shown, the total surface free energy of the flat Vermont talc (48.0 mJ/m^2) is higher than the flat Montana talc (41.4 mJ/m^2). As the Montana talc surface was found to be more hydrophobic, it is expected that the surface free energy of the Montana talc should be lower than the Vermont talc. Thus, the data presented in this table reflects the results of contact angle measurements.

Table 2.10 also compares the flat and powdered Montana and Vermont talc samples in terms of their surface free energy components. As shown, the surface free energy components of ground talc particles are different from those of original flat samples. As mentioned earlier, mechanical grinding causes considerable changes in both the Lifshitz-van der Waals component and the Lewis acid-base parameters. For example, the γ_S^{LW} for the Montana talc decreased from 35.8 mJ/m^2 on the flat surface to 31.0 mJ/m^2 on the powdered surface that is in the size range of 150 x 53 μm. It further decreased to 17.6 mJ/m^2 when the particles size was 53 μm x 0. Similarly, the γ_S^{LW} decreased from 41.4 mJ/m^2 on the flat Vermont talc surface to 21.0 mJ/m^2 on the powdered surface that is in the size range of 53 μm x 0. Also shown in Table 2.10, the value of γ_S^- somehow changed from the original flat surface to the ground surface, while the γ_S^+ remained practically unchanged. The γ_S^{AB} also decreased when the particles were pulverized. For example, the γ_S^{AB} was 6.6 mJ/m^2 on the flat Vermont talc surface, while it decreased to 3.9 mJ/m^2 on the ground Vermont talc surface. As it can be seen from the table, the value of γ_S on the Montana and Vermont talc surfaces also decreased when the samples were ground. The decrease in the value of γ_S is achieved due to the decrease in the values of both γ_S^{LW} and γ_S^{AB}.

Wu et al [28] studied the effect of pulverization on the surface properties of minerals and found that the surface of minerals become more hydrophobic upon grinding.

However, they did not discuss in detail the reason why the hydrophobicity of minerals was increased and the surface free energies were decreased after the pulverization. It becomes clear in this work that the main reason for the decrease in the values of both γ_S^{LW} and γ_S^{AB} is the creation of more hydrophobic basal plane surfaces on the ground samples.

Considering the crystal structure of talc, the talc particles have the shape of platelets due to the layer structure of the mineral. The atoms within the layers are held together by ionic bonds, while the oxygen-oxygen interlayer atoms (linked together by siloxane bonds) by weak van der Waals forces [7-9]. As a result, easy breakage takes place along the layers that are termed as the "basal planes". Since the basal planes are composed predominantly of Lifshitz-van der Waals component of surface free energy, it can be predicted that the total surface free energy (γ_S) at the basal plane surface should be lower than the total surface free energy at the edge surface. Apolar surfaces, e.g. Teflon, are known to possess only the γ_S^{LW}; therefore, their total surface free energy is usually lower than the polar surfaces that have both γ_S^{LW} and γ_S^{AB} surface free energy components (e.g. metals, hydrophilic minerals). The creation of new basal surfaces upon grinding causes a decrease in the values of γ_S^{LW} and γ_S^{AB} and hence, a decrease in the value of γ_S.

The surface free energy parameters obtained from the capillary rise measurements on various powdered talc samples are given in Table 2.11. The results show that the surface free energy (γ_S) was significantly reduced on the powdered talc samples as compared to those obtained on the flat surfaces. As shown, the γ_S decreased to a value of 30 mJ/m^2 on the Select-A-Sorb powder associated with decrease in the values of both γ_S^{LW} and γ_S^{AB}.

Figure 2.6 shows the surface free energy parameters γ_S^{LW}, γ_S^+, γ_S^- and γ_S^{AB} obtained for various flat and powdered talc surfaces, plotted as a function of advancing water contact angles (θ_a) exhibited by these surfaces. The results given in Tables 2.9 through 2.11 and Figure 2.6 show some important trends that need to be discussed. For a given talc surface, the value of γ_S^- is much higher than the value of γ_S^+ for surfaces with lower hydrophobicities. For example, at θ_a=62.3^o, γ_S^- =13.8 mJ/m^2 whereas γ_S^+ =0.8

mJ/m^2. As the surface becomes more hydrophobic, the value of γ_S^- decreases, while the value of γ_S^+ remains practically unchanged. For example, at θ_a=89.9°, γ_S^- =1.0 mJ/m^2 whereas γ_S^+ =0.9 mJ/m^2. The results presented here agree well with those reported in literature for the hydrophobic surfaces [56].

Figure 2.6 shows also that the values of Lifshitz-van der Waals component decrease as the θ_a increases. For example, γ_S^{LW} changes from 41.4 mJ/m^2 at θ_a=62.3° to 28.2 mJ/m^2 at θ_a=89.9°. As discussed above, the creation of more basal plane surfaces upon grinding causes a significant increase in the value of water contact angle and decrease in the value of γ_S^{LW} on the powdered samples. The values of γ_S^{LW} on the flat and powdered talc samples reported here (28.8 - 41.4 mJ/m^2) agree well with those reported (33.4-40.4 mJ/m^2) by Wu et al [28].

As shown in Figure 2.6, there is a general trend that the values of γ_S^{AB} decrease with increasing θ_a. The decrease in γ_S^{AB} is a direct consequence of the decrease in γ_S^- (and γ_S^+) as suggested by Eq. [2.10]. As discussed above, an increase in θ_a is achieved mainly because of the creation of additional basal plane surfaces on the ground talc surfaces. With increased basal plane surfaces, the surfaces changes from the one showing higher polarity that can readily participate in acid-base interactions with water molecules to a less polar that has little tendency to interact with the water molecules. Even though this is a general trend there are some discrepancies observed in the figure as well. For example, Mistron Vapor-P and Yellowstone powders, both of which has smaller values of water contact angles than the powdered Montana talc surface (150 x 53 μm), exhibit lower values of γ_S^{AB}. It would be expected that the more hydrophobic Montana talc surface should have a smaller value of γ_S^{AB}.

Table 2.12 gives the values of surface free energy parameters γ_S^{LW}, γ_S^+, γ_S^- and γ_S^{AB} obtained from the thin layer wicking measurements for various powdered talc surfaces, whereas Figure 2.7 shows the same parameters, plotted as a function of advancing water contact angles (θ_a) exhibited by these surfaces. The results given in Table 2.12 and Figure 2.7 obtained from the thin layer wicking measurements demonstrate somewhat different trend compared to those determined using the capillary rise technique. As shown in Figure 2.7, the values of γ_S^-, γ_S^+ and γ_S^{AB} are nearly the same

over the whole range of water contact angle, even though some measurable differences can be observed on the value of γ_S^-. Also shown, the decrease in the value of γ_S is primarily attributed to the decrease in the value of γ_S^{LW}. The γ_S^{AB} contributes in this reduction to some extend, even though its contribution is small as compared to the capillary rise technique.

The results presented in Tables 2.11 and 2.12 show that the values of γ_S obtained from the thin layer wicking measurements were lower compared to those obtained from the capillary rise measurements. The total surface free energies of powdered talc samples obtained from the thin layer wicking measurements are in the range from 22.1 mJ/m^2 to 28.0 mJ/m^2, whereas it changes from 28.2 mJ/m^2 to 45 mJ/m^2 determined using the capillary rise technique.

The difference between the values of γ_S determined using two methods should be attributed to the values of the contact angles measured. As discussed earlier, it is probable that the lower values of contact angles were obtained from the capillary rise measurements on the ultrafine talc powders due to the bed disturbances during measurements; therefore, the values of γ_S^{LW} and γ_S^{AB} determined using this technique were higher. The thin layer wicking technique, however, gave considerably higher values of contact angles with all of the test liquids used. The values of γ_S^{LW} and γ_S were especially lower. It is believed that the thin layer wicking is a more convenient method of measuring contact angles on the very fine talc powders and characterizing these powders in terms of their surface free energy parameters.

Table 2.12 also gives the values of surface free energy parameters γ_S^{LW}, γ_S^+, γ_S^- and γ_S^{AB} obtained from the thin layer wicking measurements for the Select-A-Sorb talc sample that is exposed to water vapor for 24 hours. As shown, after exposing the surface of Select-A-Sorb talc to water vapor, the values of surface free energy components slightly increased compared to those obtained on the unexposed surface. The change in the surface free energy parameters, however, is small, suggesting that the effect of equilibrium spreading pressure of water vapor on the talc surface is negligible. The surface free energy of Select-A-Sorb powder increased from 22.1 mJ/m^2 to only 23 mJ/m^2 after the powder was exposed to the water vapor for 24 h. The results given in this

table clearly show that the vapors of high-energy liquid, e.g. water, do not adsorb on the low free energy talc surface.

The results presented throughout this work have consistently demonstrated that the surface of talc is predominantly basic, but there are also few acidic sites. As shown in Figure 2.6, the basal planes of talc are made up of O atoms that are linked together by Si-0-Si bonds, while the edges are composed of MgOH, SiOH and the other substituted cations, e.g. Al^{3+}, Fe^{2+} [7-9]. Among those MgOH is slightly basic, while the other surface ions on the edge surfaces are acidic in character. The type and degree of cation substitution on the edge surfaces can also affect the surface characteristics of talc. For example, if a certain portion of Si is substituted by Al ions, then the surface acidity of the edge surfaces should decrease. Thus, overall the talc surface becomes more basic. ESCA (Electron Spectroscopy for Chemical Analysis) measurements were conducted on Mistron-100 and Select-A-Sorb talc powders to explore the elemental composition, chemical state information and surface characteristics that lead to the surface basicity of talc. This technique, also known as x-ray photoelectron spectroscopy (XPS), provides a quantitative elemental analysis of the top 1-20 nm of a solid surface [57, 58].

Figure 2.9 and 2.10 show a wide scan ESCA spectrum obtained on the Select-A-Sorb powders and Mistron-100, respectively. As shown, the ESCA spectrum gave Mg, Si, O, Al, C, Na and F peaks associated with their corresponding binding energies on both talc surfaces. The Mg, Si and O elements are the main constituents forming the crystal lattice of talc which has a chemical formula of $Mg_3Si_4O_{10}(OH)_2$. Al, however, is placed in the crystal structure as a result of substitution with Si atoms [5]. C is probably found as an impurity, adsorbed on the talc surface from the ambient in the form of organic carbon [59]. Even though, the samples were dried at 110 ^{o}C to remove the moisture, the heating was not sufficient to remove the C containing impurities from the talc surface. Hydrogen can not be detected by ESCA method, so no peak representing H was observed in these measurements.

The elemental analysis results of talc samples from the ESCA measurements showed that almost 20% of the Si atoms is substituted by Al as shown in Table 2.13. Also shown in the table is the theoretical chemical composition of talc. As shown, the percentage of Mg defined in the Select-A-Sorb talc (9.3%) is slightly higher than that

determined in the Mistron-100 talc (8.3%), while the degree of Al substitution on both Select-A-Sorb and Mistron-100 powders is the same. As discussed above, the Mg and Al atoms contribute to the basicity of talc surface. The results given in Table 2.12 showed that the surface of Select-A-Sorb powder is slightly more basic than the surface of the Mistron-100. The values of γ_S^- on the Select-A-Sorb and Mistron-100 powders as determined in the present work were 6.5 mJ/m^2 and 6.1 mJ/m^2, respectively. Thus, the data given in Table 2.13 confirm the surface free energy components that are determined using the thin layer wicking technique (Table 2.12).

The results given in Tables 2.9 through 2.12 show that the estimated values of γ_S are in the range of 21.6 to 53.1 mJ/m^2, depending on the particle size (either in the form of flat or powder) and the technique used. The value of γ_S is higher on the flat surfaces and it decreases on the powdered surfaces, along with increase in the value of contact angles. For example, the value of γ_S is 48.0 mJ/m^2 at θ_a=62.3^o, while it is 22.1 mJ/m^2 at θ_a=89.4^o. In fact, both γ_S^{LW} and γ_S^- and γ_S^+ are responsible for a decrease in the value of γ_S or an increase in the value of advancing water contact angle. As shown in Figure 2.6, as the values of γ_S^{LW} and γ_S^{AB} components decrease, γ_S decreases accordingly. As shown in Table 2.12 and Figure 2.7, however, the decrease in the value of γ_S is mainly achieved due to the decrease in the value of γ_S^{LW}, even though the γ_S^{AB} contributes in this reduction to some extend. Note also that the value of γ_S^{AB} may become zero on a hydrophobic or a monopolar surface; on the other hand, γ_S^{LW} never becomes zero. Overall, the surface hydrophobicity is a function of the value of γ_S, as well as its components.

2.4 CONCLUSIONS

Contact angle measurements were conducted on flat and powdered surfaces to determine the surface free energy components (γ_S^+, γ_S^-, γ_S^{AB} and γ_S^{LW}) of talc samples using the van Oss, Chaudhury and Good (VCG) thermodynamic approach. The results showed that there is a relationship between particle size and the measured contact angles. As the particle size decreases water contact angle increases, which can be attributed due to the fact that more nonpolar basal plane surfaces are created.

The results also showed that the surface of talc contains both basic and acidic sites. However, the number of basic sites is much larger than the number of acidic sites as defined from the contact angle measurements and by the application of VCG equation. The ESCA measurements also confirmed the surface basicity of talc surface as defined from the contact angle measurements.

As a general trend, the γ_S^{AB} and γ_S^{LW} components of surface free energy decrease with decreasing particle size, and so does the value of γ_S. A linkage between particle hydrophobicity and surface free energy components was established. The more the hydrophobic surface is the lower the γ_S is. However, this is associated with decreases both in the values of γ_S^{LW} and γ_S^{AB}.

2.5 REFERENCES

1. Good, R. J., and van Oss, C. J., in *Modern Approaches to Wettability: Theory and Applications*, Eds: M. E. Schrader, and G. Loeb, Plenum Press, New York, pp. 1-27, 1992.
2. Janczuk, B, Wojcik, W., Zdziennicka, A., *J. of Colloid and Interface Science,* 157, 384-393, 1993.
3. Padday, J. F., (Ed), *Wetting, Spreading, and Adhesion*, Academic Press, New York, 1978.
4. Zisman, W. A., in: *Handbook of Adhesives*, Skeist, I., Ed: van Nostrand, NewYork, Chapter 3, 1977.
5. Yariv, S., Wettability of Clay Minerals, in: *Modern Approaches to Wettability: Theory and Applications*, Eds: M. E. Schrader, and G. Loeb, Plenum Press, New York, pp. 279-326, 1992.
6. Chander, S., Wie, J. M. and Fuerstenau, D. W., in: *Advances in Interfacial Phenomena*, Ed: P. Somasundaran, AIChE Series No. 150, New York, pp.183-188, 1975.
7. Fuerstenau, M. C., Lopez-Valdiviezo, A., and Fuerstenau, D.W., *Int. J. of Mineral Proc.*, 23, 161-170, 1988.
8. Rayner, J. H., and Brown, G., *Clays and Clay Minerals*, Vol. 21, 103-114, 1973.

9. Ciullo, P. A., in: *Industrial Minerals and Their Uses-A Handbook and Formulary*, Ed: P. A. Cuillo, Noyes Publications, New Jersey, 1996.
10. Pukansky, B., in*: Polypropylene: Structure, Blends and Composites*, Ed: J. Karger-Kocsis, Vol. 3, pp. 1, Chapman and Hall, London, 1995.
11. Schlumpf, H. P., *Synthetis,* 12, 31, 1981.
12. Nakatsuka, T., *Polym. Sci. Technol.,* 27, 51, 1985.
13. Fowkes, F.M., *Industrial and Engineering Chemistry*, 56/12, 40, 1964.
14. Fowkes, F.M., J. of Adhesion, 4, 153, 1972.
15. Van Oss, C. J., Chaudhury, M. K., and Good, R. J., J. *Separation Sci. and Technology,* 22, 1, 1987.
16. Van Oss, C. J., Good, R. J., and Chaudhury, M. K., *Langmuir*, 4, pp. 884-891, 1988.
17. Van Oss, C. J., Chaudhury, M. K., and Good, R. J., *J. Colloid Interface Science*, 128, 313, 1989.
18. Neumann, A. W. and Good, R.J., *Techniques of Measuring Contact Angles, Surface and Colloid Science*, Volume II, Experimental Methods, Eds: R.J. Good and R. R. Stromberg, Plenum Pres, New York, 1979.
19. Fuerstenau, D. W., *Mining Engineering*, Transactions AIME, December, pp. 1367-1367, 1957.
20. Leja, J., *Surface Chemistry of Froth Flotation*, Plenum Press, New York, 1982.
21. Yoon, R.-H., *Aufbereitungs-Technik*, 32, 474, 1991.
22. Yoon, R.-H., and Ravishankar, S. A., *J. Colloid Interface Science*, 179, 391, 1996.
23. Yoon, R.-H., and Pazhianur, R., *Colloid Surfaces*, 1999.
24. Bruil, H. G., and van Aartsen, J. J., *Colloid & Polymer Science*, 252, pp. 32-38, 1974.
25. Hansford, D. T., Grant, D. J. W., and Newton, J. M., *J. C. S. Faraday I*, 76, 2417-2431, 1980.
26. Crawford, R., Koopal, L. K. and Ralston, J., *Colloids and Surfaces*, 27, 57-64, 1987.
27. Van Oss C.J., Griese, R.F. Jr., Li, Z., Murphy, K., Norris, J., Chaudhury, M. K., and and Good, R. J., J. *Adhesion Sci. and Technology*, Vol. 6, No.4, 413-428, 1992.

28. Wu, W., Griese, R.F. Jr., and van Oss C.J., *Powder Technology*, 89, 129-132, 1996.
29. Fowkes, F. M., in *Surfaces and Interfaces*, Eds: J. J. Burke, Syracuse University Press, 1967.
30. Laskowski, J. S., and Kitchener, J. A., *J. of Colloid and Interface Science*, 29, 670, 1969
31. Fowkes, F.M., and Mostafa, M.A., *Industrial and Engineering Chemistry Prod. Res. Dev.*, 17, 3, 1978.
32. Fowkes, F.M., in: *Physicochemical Aspects of Polymer Surfaces*, Ed: K.L. Mittal, vol. 2, p. 583, Plenum Press, New York, 1983.
33. Fowkes, F.M., *J. Adhesion Sci. Technol*., 4, 669, 1990.
34. Van Oss, C. J., Good, R. J., and Chaudhury, M. K., *J. of Colloid and Interface Science*, 111, pp. 378, 1986.
35. Van Oss, C. J., Chaudhury, M. K., and Good, R. J., *J. of Colloid and Interface Science*, 128, 313, 1988.
36. Van Oss, C. J., Giese, R.F., Good, R. J., *Langmuir*, 6, pp. 1711-1713, 1990.
37. Van Oss, C. J., Chaudhury, M. K., and Busscher, H., *J. of Dispersion Sci. Technol.*, 11, 77, 1990.
38. Dupré, A., 1869. *in Ref. 40*.
39. Young, T., 1805. *in Ref. 40*.
40. Van Oss, C. J., *Interfacial Forces in Aqueous Media*, Marcel Decker Inc., New York, 1994.
41. Berg, J. C., *Nordic Pulp and Paper Research Journal*, 1, 75-85, 1993.
42. Yordan, J. L. and Yoon, R.- H., *J. of Colloid and Interface Science,* Vol. 146, No. 2, pp. 101-108, 1991.
43. Adamson, A. W., *Physical Chemistry of Surfaces*, 5th ed., John Wiley and Sons, 1990.
44. Fowkes, F. M., McCarthy, D. C., and Mostafa, M. A., *J. of Colloid and Interface Science,* 78, 200, 1980.
45. Busscher, H. J., Kim, K. G. A., Van Silfout, G. A. M., and Arends, J., *J. of Colloid and Interface Science,* 114, 307, 1986.

46. Bellon-Fontaine, M.-N. and Cerf, O., J. *Adhesion Sci. and Technology,* 4, 475, 1990.
47. Adamson, A. W. and Gast, A.P., *Physical Chemistry of Surfaces,* 6th ed., John Wiley and Sons, 1997.
48. Washburn, E. W., 1921, *Physical Review*, 1, pp. 273 (in Ref. 24).
49. Davies, J. T., Rideal, E. K., *Interfacial Phenomena*, (New York), 423 (1963).
50. Van Oss, C. J., Wu, W., and Griese, R.F. Jr., *Particulate Science and Technology*, 11:193-198, 1993.
51. Spagnolo, D. A., Maham, Y., and Chuang, K. T., *J. Phys. Chem.*, 100, pp. 6626-6630, 1996.
52. Weast, R. C., Astle, M. J., (Eds.), *Handbook of Physical Chemistry*, 61st ed., CRS Press, Inc., Boca Baton, FL, 1981.
53. Zisman, W. A., *Advances in Chemistry*, No.43, ACS, 1964.
54. Neumann A. W., *Adv. Colloid Interface Sci.*, 4, 105, 1974.
55. Good, R. J., in: *Contact Angle, Wettability, and Adhesion*, Ed: K. L. Mittal, VSP, Utrecht, 1993.
56. Pazhianur, R., *Ph.D. Thesis*, Virginia Tech, 1999.
57. Iston, W. K., in: *Surface Analysis of Paper*, Eds: T. E. Conners and S. Banerjee, CRC Pres, 1995.
58. Carlson, T. A., *Photoelectron and Auger Spectroscopy*, Plenum Press, New York and London, 1975.
59. McCafferty, E., and Wightman, J. P., *Surf. Interface Anal.*, 26, pp. 549-564, 1998.

Table 2.1. Values of the surface tension components (in mJ /m^2) and of the viscosities (in poise) of the liquids used in the capillary rise and thin layer wicking experiments

Liquid	γ_L	γ_L^{LW}	γ_L^{AB}	γ_L^+	γ_L^-	η
Hexane	18.4	18.4	0	0	0	0.00326
Heptane	20.3	20.3	0	0	0	0.00409
Octane	21.6	21.6	0	0	0	0.00542
Decane	23.8	23.8	0	0	0	0.00907
Dodecane	25.35	25.35	0	0	0	0.01493
Cyclohexane	25.5	25.5	0	0	0	0.00912
Benzene	28.9	27.1	0	0	2.8	0.00604
1-Bromonaphthalene	44.4	44.4	0	0	0	0.0489
Methylene iodide	50.8	50.8	0	0	0	0.028
Ethylene glycol	48.0	29.0	19.0	1.92	47.0	0.199
Formamide	58.0	39.0	19.0	2.28	39.6	0.0455
Glycerol	64.0	34.0	30.0	3.92	57.4	14.90
Water	72.8	21.8	51.0	25.5	25.5	0.010

Table 2.2. Equilibrium Contact Angles of Various Liquids on Flat Montana and Vermont Talc Surfaces Measured Using Sessile Drop Technique (at 20±2 ^oC)

Liquid	Montana	Vermont
Water	51.5±3.0	50.0±2.5
Glycerol	44.0±2.5	43.5±2.5
Formamide	39.5±3.0	38.0±3.0
Methylene iodide	33.0±2.0	29.0±2.0
1-Bromophthalene	17.0±3.0	14.0±3.0
Heptane	Spreads	Spreads

Table 2.3. Contact Angles of Various Liquids on Flat Montana and Vermont Talc Surfaces Measured Using Wilhelmy Plate Technique (at 20±2 ^{o}C)

Liquid	Montana		Vermont	
	θ_a	θ_r	θ_a	θ_r
Water	69.7±2.0	39.0±2.5	62.3±2.0	37.6±2.5
Formamide	50.8±2.3	33.9±2.7	40.5±2.5	27.1±2.8
Methylene iodide	47.2±2.5	30.8±2.8	36.3±2.7	24.2±3.0

Table 2.4. Advancing Contact Angles of Various Liquids on Powdered Talc Samples Obtained from Capillary Rise Method (at 20±2 ^{o}C)

Talc Sample	Water	Formamide	1-Bromophthalene
Yellowstone	69.7±5.3	43.7±5.0	30.0±4.7
Mistron-100	74.0±3.8	47.9±4.5	31.0±4.0
Mistron Vapor-P	77.9±4.7	58.7±4.8	51.6±4.6
Select-A-Sorb	89.9±2.4	61.4±4.0	53.5±3.5

Table 2.5. Average pore size (r^*) determined by thin layer wicking on various talc powders (at 20±2 ^{o}C)

Talc Sample	Particle Size	r^* (nm)
Mistron-100	d_{50}=3.5 μm	294.7
Mistron Vapor-P	d_{50}=3.0 μm	538.6
Yellowstone	d_{50}=12.5 μm	626.7
Select-A-Sorb	d_{50}=3.4 μm	807.4
Montana-ROM	(53 μm x 0)	1333.0
Vermont-ROM	(38 μm x 0)	3093.0

Table 2.6. Contact angles θ (deg) of various liquids on powdered talc samples measured using thin layer wicking technique (at 20±2 °C)

	1-Br	MI	W	FO	EG
Mistron-100	45.4±1.4	58.1±1.5	82.0±1.8	62.9±2.0	49.5±1.9
Yellowstone	63.4±1.8	72.2±1.6	84.5±2.0	67.2±1.8	65.2±1.8
Mistron Vapor-P	68.7±1.6	74.8±1.5	85.5±1.6	72.0±1.5	71.5±1.8
Select-A-Sorb	74.6±1.0	78.6±1.0	89.4±0.4	77.2±0.9	74.3±0.8
Montana-ROM	74.0±2.0	80.0±1.8	86.6±1.8	79.6±1.9	78.2±1.7
Vermont-ROM	69.8±2.2	73.6±2.0	84.1±2.5	73.4±2.1	70.4±2.0

1-Br=1-Bromonapthalene, MI=Methylene Iodide, W=Water, FO=Formamide, EG=Ethylene glycol

Table 2.7. Effect of Particle Size on the Values of Water and Formamide Contact Angles for Montana and Vermont Talc Samples

Sample	Advancing Contact Angle (θ_a)					
	Water			Formamide		
	Flat	150x53 μm[(1)]	53 μmx0[(2)]	Flat	150x53 μm[(1)]	53 μmx0[(2)]
Montana	69.7	82.3	86.5	49.8	56.1	79.6
Vermont	62.3	74.2	84.1[(3)]	39.4	48.0	73.4[(3)]

(1) Obtained from capillary rise measurements.
(2) Obtained from thin layer wicking measurements.
(3) 38 μm x 0 particle size was used.

Table 2.8. Effect of Water Exposure on the Values of Contact Angles of Select-A-Sorb Talc Powder Measured Using Thin Layer Wicking Technique

Liquid	Advancing Contact Angle (θ_{adv})	
	Before Exposure	After Exposure [(*)]
1-Bromonaphthalene	74.6±1.0	72.1±1.4
Methylene Iodide	78.6±1.0	75.3±1.7
Water	89.4±0.4	87.5±0.4
Formamide	77.2±0.9	76.5±1.5
Ethylene Glycol	74.3±0.8	71.7±1.8

[(*)] Powder was exposed to water vapor for 24 h.

Table 2.9. Surface Free Energy and its Components of Montana and Vermont Talc Samples Calculated from θ_{eq} Measured Using Sessile Drop Technique

Sample	Liquids	Surface Free Energy (mJ/m^2)				
		γ_S^{LW}	γ_S^+	γ_S^-	γ_S^{AB}	γ_S
Montana Talc	MI / W / F	42.9	0.2	27.4	4.7	47.6
	MI / W / G	42.9	1.0	21.4	9.3	52.2
Vermont Talc	MI / W / F	44.6	0.1	28.4	3.4	48.0
	MI / W / G	44.6	0.8	22.7	8.5	53.1

MI: Methylene iodide, W:Water, F:Formamide, G:Glycerol.

Table 2.10. Surface Free Energy Components of Flat and Powdered Montana and Vermont Talc Samples

	Flat [1]				
	γ_s^{LW}	γ_s^+	γ_s^-	γ_s^{AB}	γ_s
Montana	35.8	0.7	11.1	5.6	41.4
Vermont	41.4	0.8	13.8	6.6	48.0
	Powdered (150 x 53 μm) [2]				
	γ_s^{LW}	γ_s^+	γ_s^-	γ_s^{AB}	γ_s
Montana	31.0	1.5	3.3	4.5	35.5
Vermont	33.7	1.8	6.1	6.6	40.3
	Powdered (53 μm x 0) [3]				
	γ_s^{LW}	γ_s^+	γ_s^-	γ_s^{AB}	γ_s
Montana	17.5	0.4	10.6	4.1	21.6
Vermont [4]	20.9	0.4	9.4	3.9	24.8

[1] *Obtained from Wilhelmy plate measurements*
[2] *Obtained from capillary rise measurements*
[3] *Obtained from thin layer wicking measurements*
[4] *38 μm x 0 particle size fraction was used.*

Table 2.11. Surface Free Energy and its Components of Powdered Talc Samples Obtained from Capillary Rise Measurements

Talc Sample	Surface Free Energy, mJ/m^2				
	γ_s^{LW}	γ_s^+	γ_s^-	γ_s^{AB}	γ_s
Yellowstone	38.7	1.2	8.3	6.3	45.0
Mistron 100	38.3	0.9	6.4	4.8	43.1
Mistron Vapor-P	29.2	1.0	7.6	5.5	34.7
Select-A-Sorb	28.2	0.9	1.0	1.9	30.1

Table 2.12. Surface Free Energy and its Components of Powdered Talc Samples Obtained from Thin Layer Wicking Measurements

Talc Sample	Surface Free Energy, mJ/m^2				
	γ_s^{LW}	γ_s^+	γ_s^-	γ_s^{AB}	γ_s
Mistron 100	29.7	0.5	6.1	3.5	33.2
Yellowstone	23.3	1.1	5.8	5.1	28.4
Mistron Vapor-P	20.6	0.8	7.3	4.8	25.4
Select-A-Sorb	17.8	0.7	6.5	4.3	22.1
Select-A-Sorb [(1)]	19.0	0.5	7.9	4.0	23.0

[(1)] *Particles were exposed to water vapor for 24 h.*

Table 2.13. Chemical Composition of Mistron-100 and Select-A-Sorb Powders as Determined from ESCA Measurements

Element	Mistron-100	Select-A-Sorb	Theoretical Composition of Talc
Mg	8.29	9.30	19.23
Si	19.26	19.94	29.62
O	56.04	58.92	50.62
H	-	-	0.53
Al	5.58	5.37	-
C	10.14	6.16	-
F	0.35	-	-
Na	0.34	0.31	-
Total	100.00	100.00	100.00

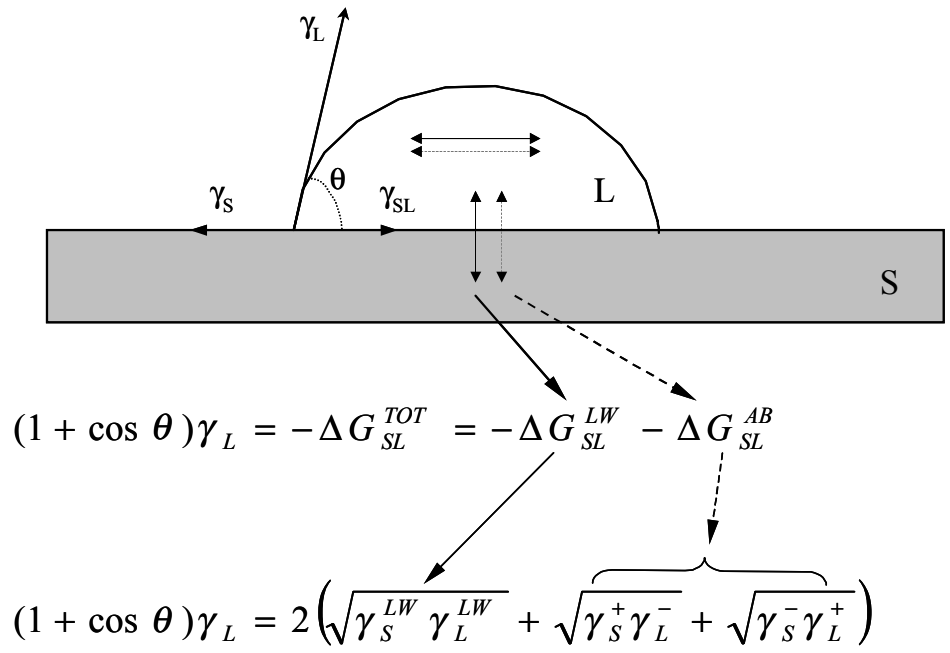

Figure 2. 1. Schematic representation of the contact angle formed between a liquid droplet and a solid surface. cosθ is a measure of the equilibrium between the molecules of liquid L (horizontal arrows) and adhesion between liquid L and solid S (vertical arrows). Apolar energies are indicated by solid horizontal or vertical lines and arrows; polar (Lewis-acid base) energies are shown by dashed horizontal or vertical lines and arrows (40).

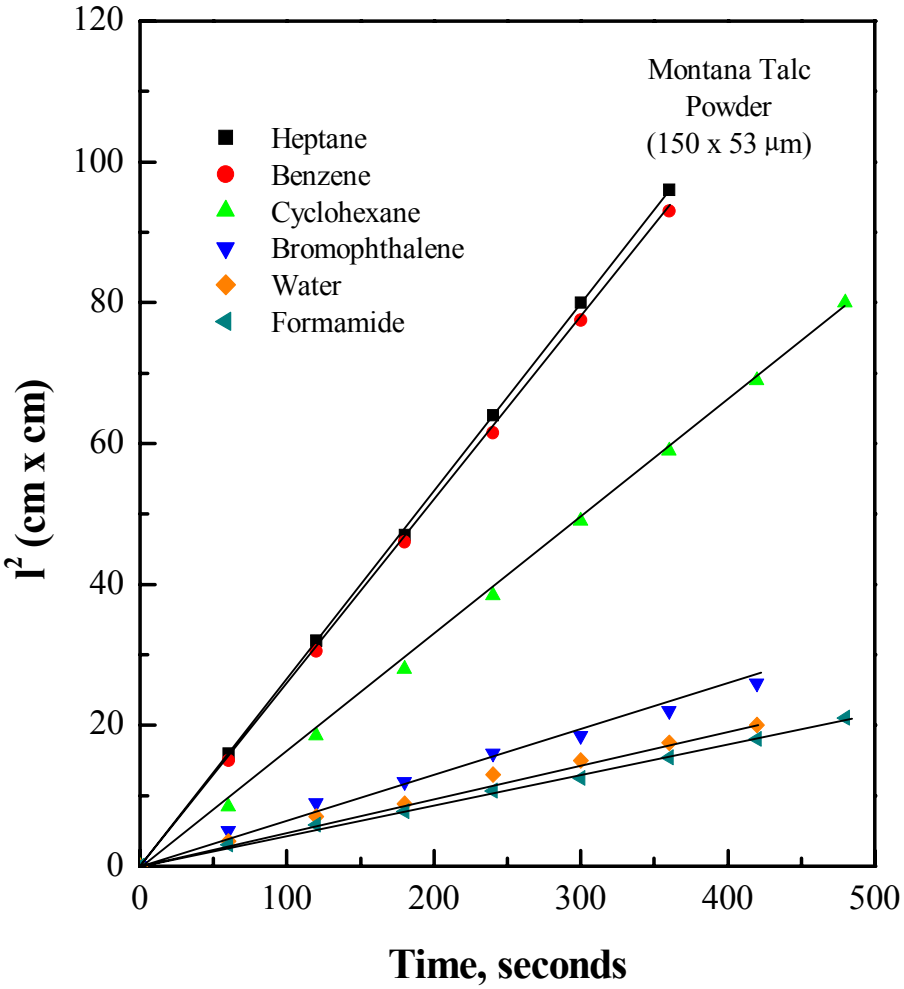

Figure 2.2. Wetting of Montana talc powder by different liquids in capillary rise at 20 °C.

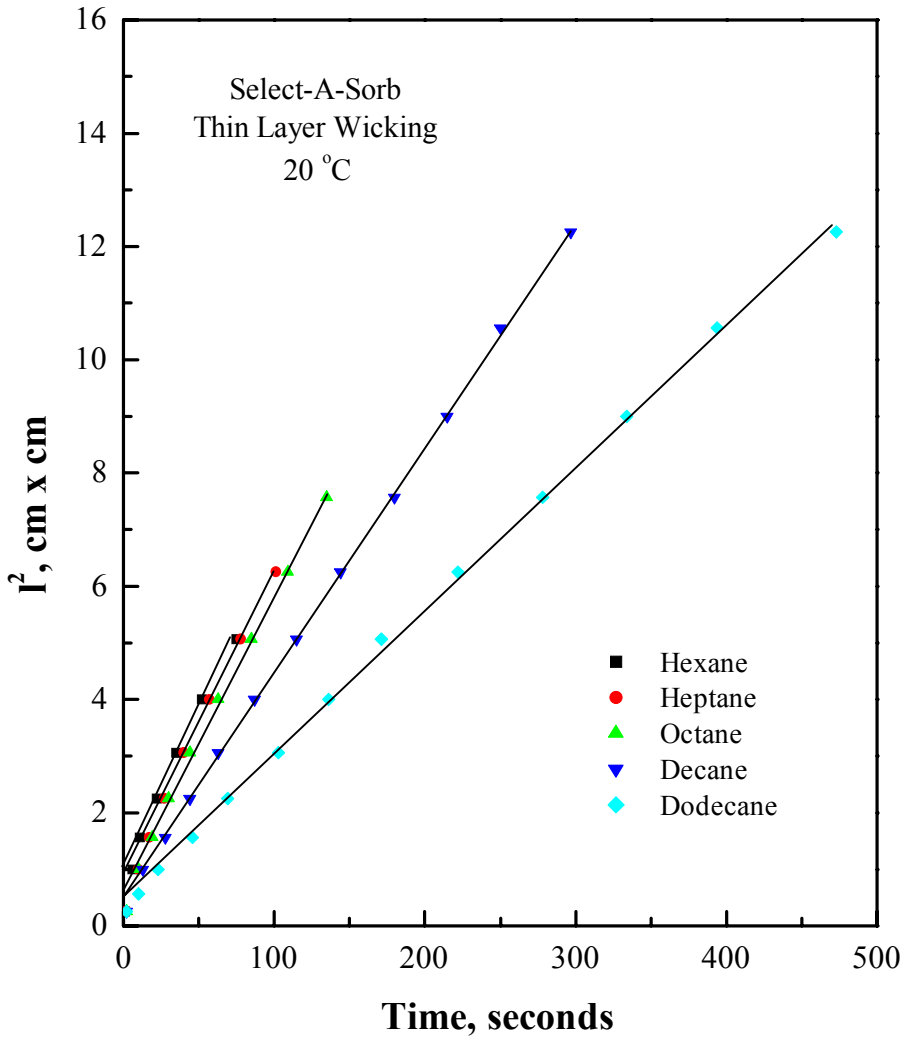

Figure 2.3. Wetting of Select-A-Sorb talc powder with low-energy liquids (alkanes) in the thin layer wicking experiments measured at 20 °C.

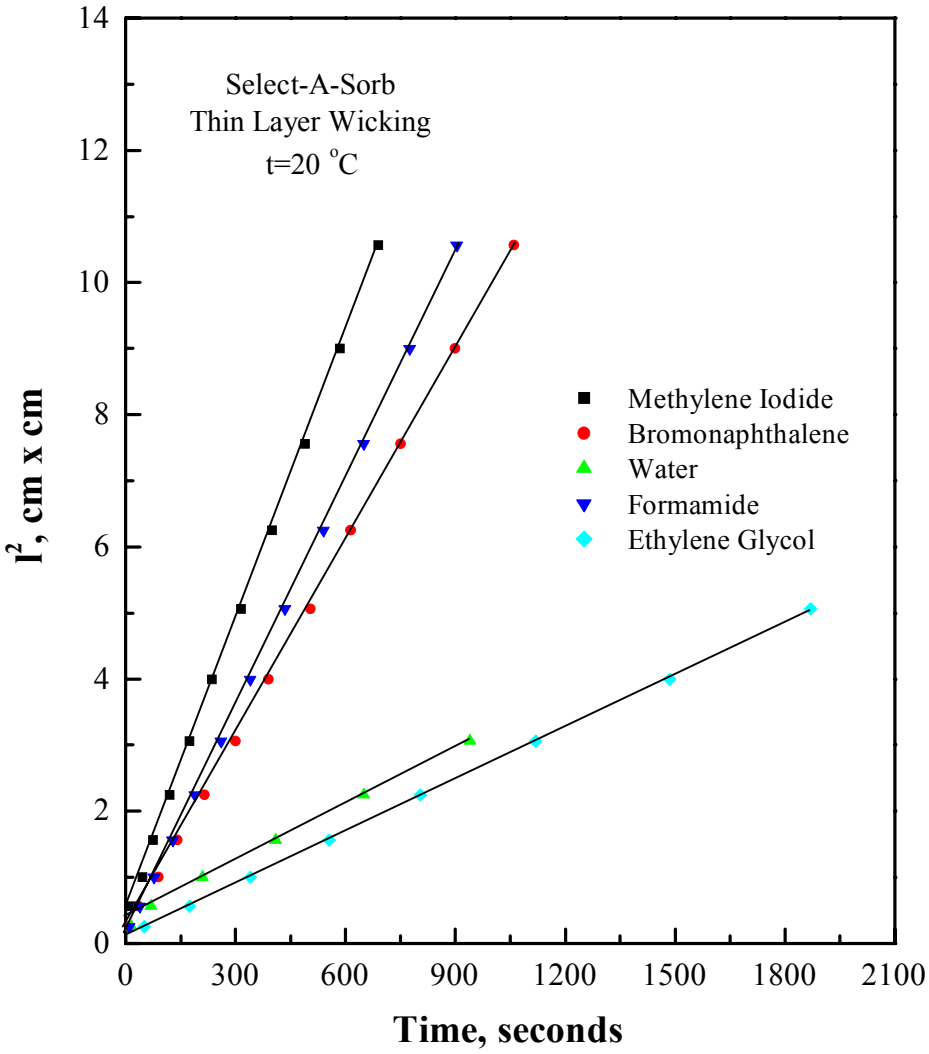

Figure 2.4. Wetting of Select-A-Sorb talc powder with high-energy liquids in the thin layer wicking experiments measured at 20 °C.

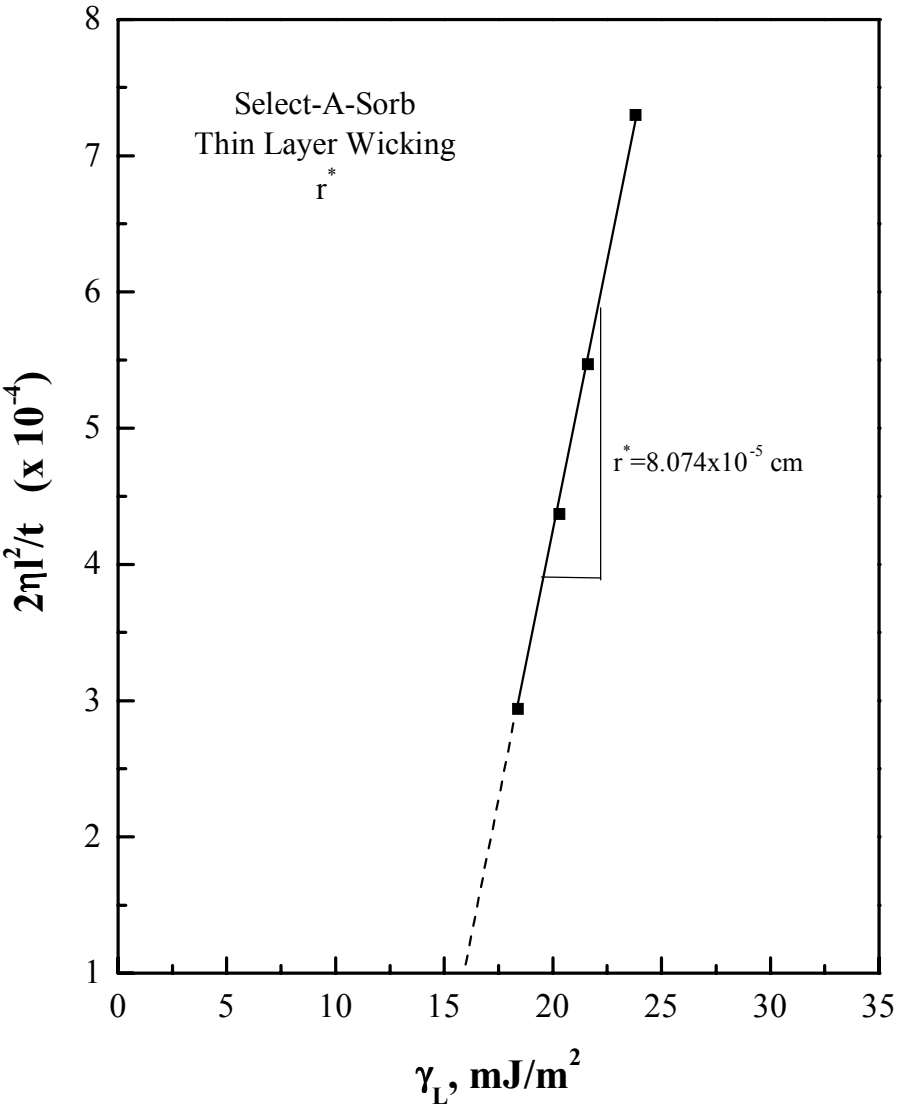

Figure 2.5. Plot of $2\eta l^2/t$ vs. γ_L obtained from thin layer wicking on Select-A-Sorb talc powder with the low-energy liquids (alkanes).

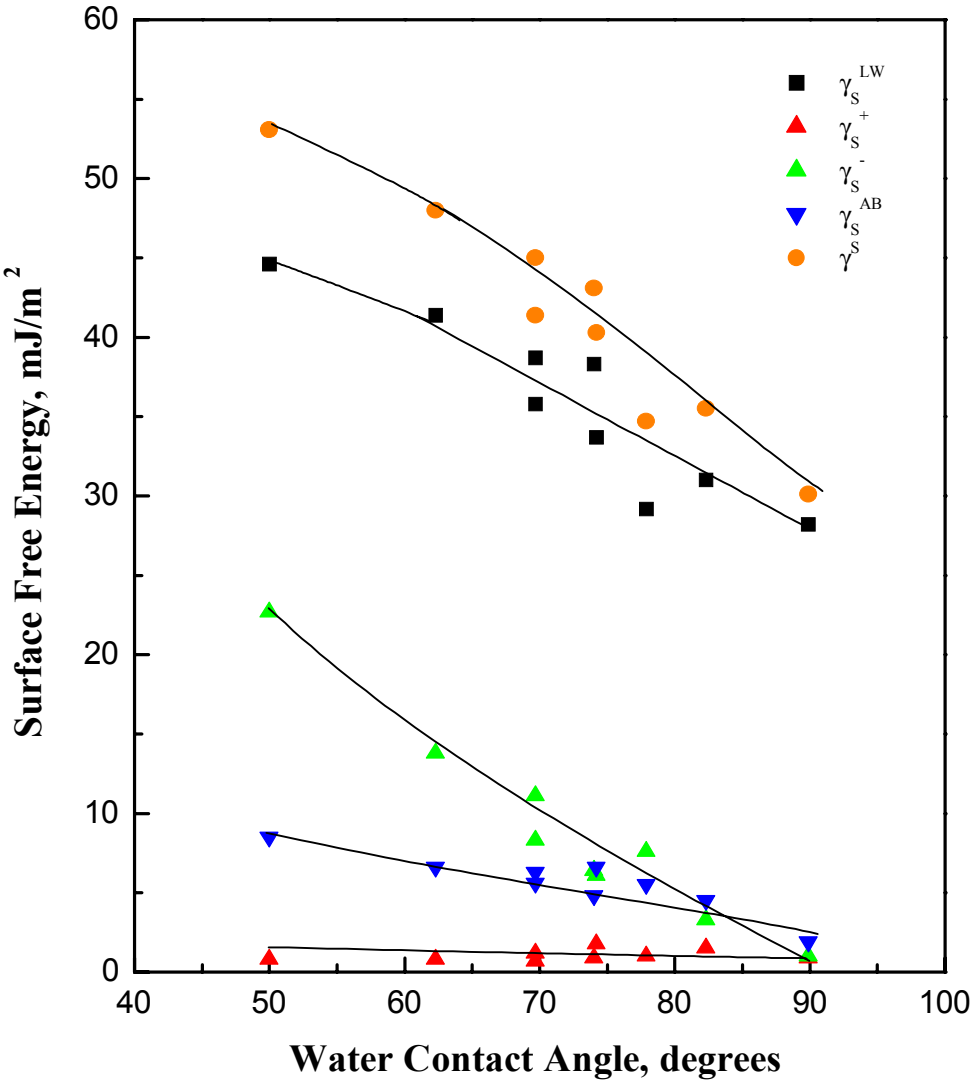

Figure 2.6. The Surface Free Energy Components of Various Flat and Powdered Talc Samples Determined Using Wilhelmy Plate and Capillary Rise Techniques, Plotted as a Function of Advancing Contact Angle, θ_a.

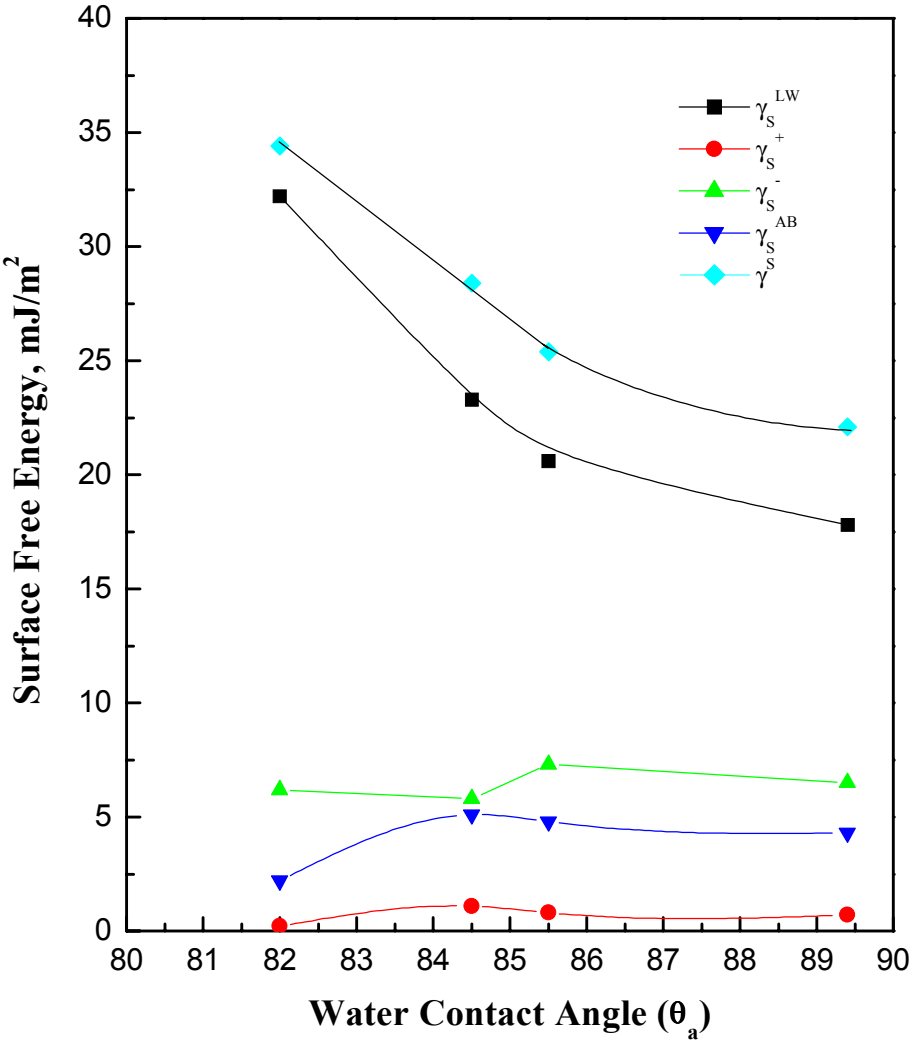

Figure 2.7. The Surface Free Energy Components of Various Powdered Talc Samples Determined Using Thin Layer Wicking Technique, Plotted as a Function of Advancing Contact Angle, θ_a.

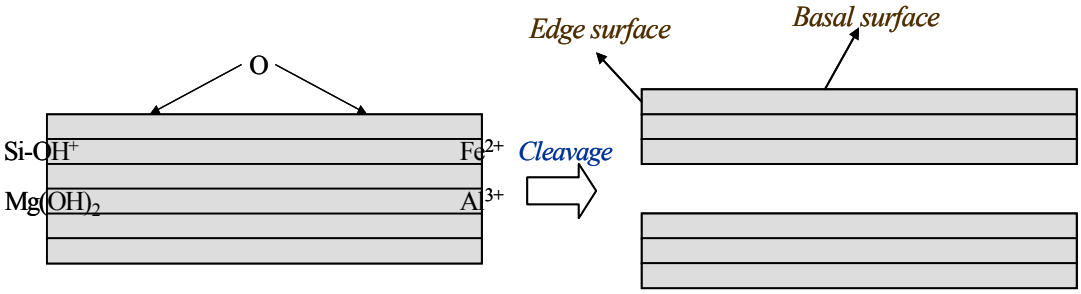

Figure 2.8. Schematic representation of the cleavage of talc layers and creation of basal plane surfaces by grinding.

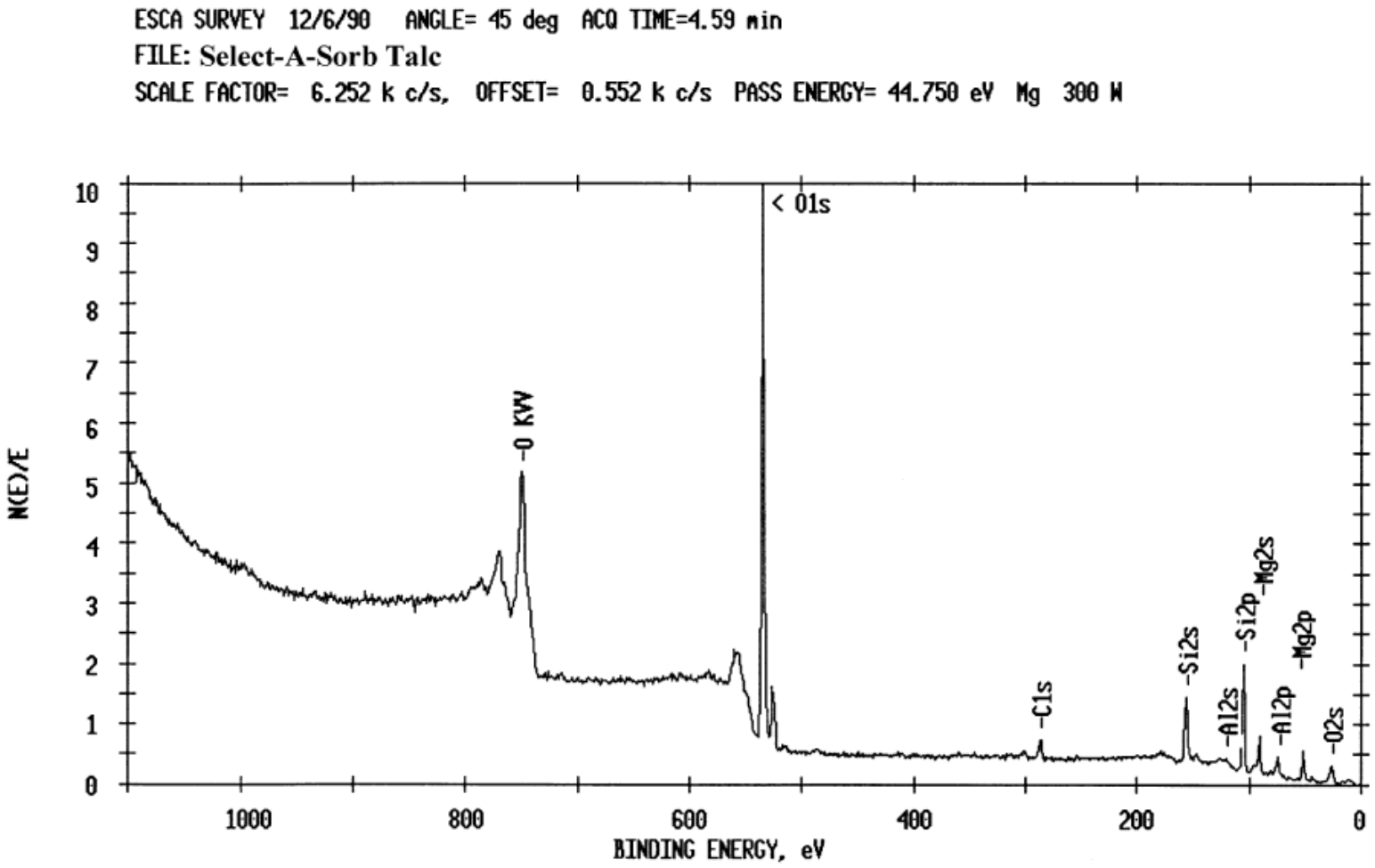

Figure 2.9. ESCA spectrum for the Select-A-Sorb talc powder.

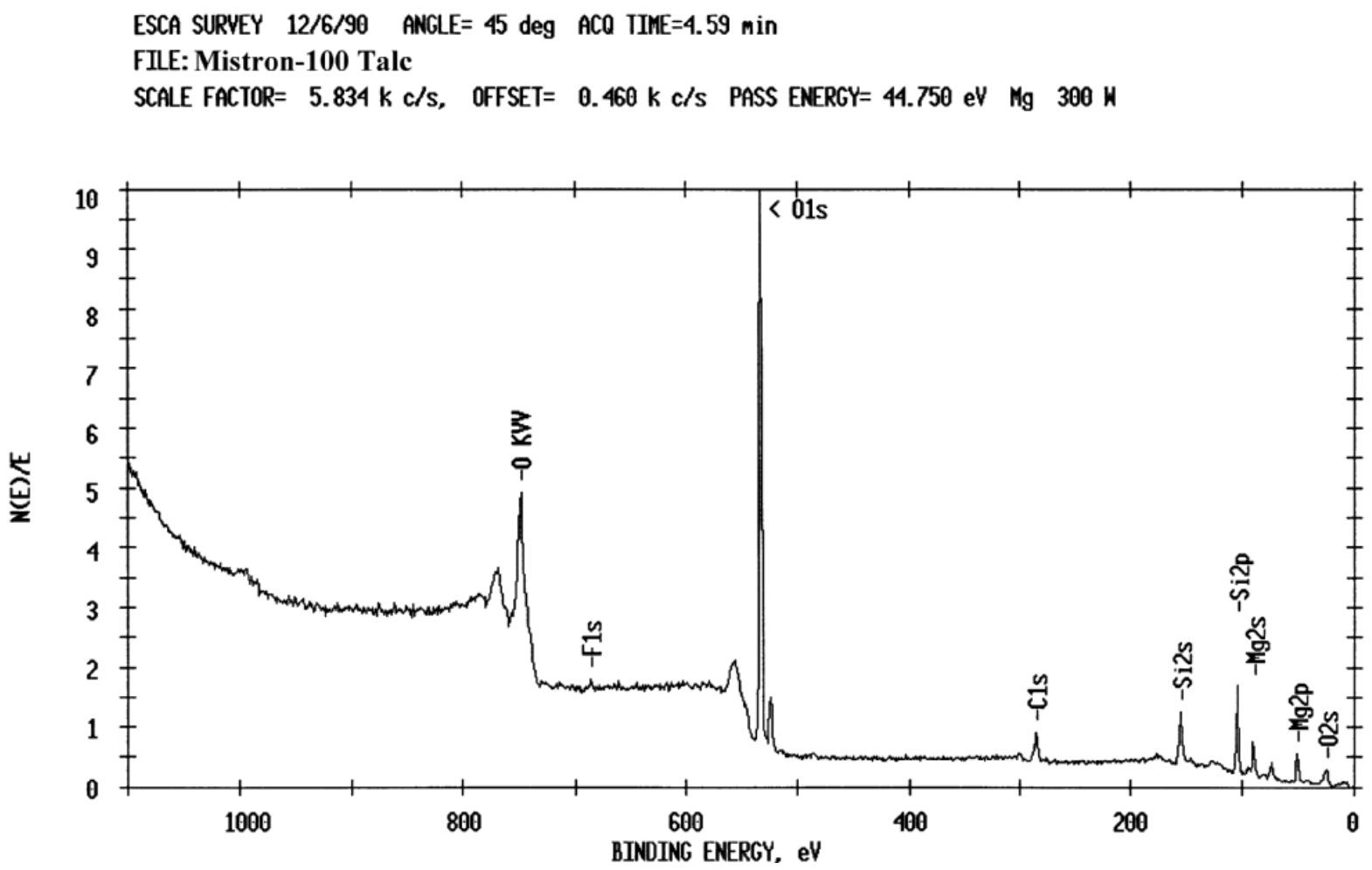

Figure 2.10. ESCA spectrum for the Mistron-100 talc powder.